

## GALAXY CLUSTERS AS A PROBE OF EARLY DARK ENERGY

UJJAINI ALAM

ISR-1, ISR Division, Los Alamos National Laboratory, Los Alamos, NM 87545, USA

ZARIJA LUKIĆ

T-2, T Division, Los Alamos National Laboratory, Los Alamos, NM 87545, USA

SUMAN BHATTACHARYA

T-2, T Division, Los Alamos National Laboratory, Los Alamos, NM 87545, USA

*Draft version September 4, 2018*

### ABSTRACT

We study a class of early dark energy (EDE) models, in which, unlike in standard dark energy models, a substantial amount of dark energy exists in the matter-dominated era. We self-consistently include dark energy perturbations, and show that these models may be successfully constrained using future observations of galaxy clusters, in particular the redshift abundance, and the Sunyaev-Zel'dovich (SZ) power spectrum. We make predictions for EDE models, as well as  $\Lambda$ CDM for incoming X-ray (eROSITA) and microwave (South Pole Telescope) observations. We show that galaxy clusters' mass function and the SZ power spectrum will put strong constraints both on the equation of state of dark energy today and the redshift at which EDE transits to present-day  $\Lambda$ CDM like behavior for these models, thus providing complementary information to the geometric probes of dark energy. Not including perturbations in EDE models leads to those models being practically indistinguishable from  $\Lambda$ CDM. An MCMC analysis of future galaxy cluster surveys provides constraints for EDE parameters that are competitive with and complementary to background expansion observations such as supernovae.

*Subject headings:*

### 1. INTRODUCTION

Over the last decade, observational evidence has mounted in favor of dark energy, the mysterious component which dominates the energy content of the universe at present, and causes the expansion of the universe to accelerate (Kowalski *et al.* 2008; Komatsu *et al.* 2009). The nature of dark energy is one of the most tantalizing mysteries of present day cosmology. The simplest model for dark energy, the cosmological constant, fits the current data well (Kowalski *et al.* 2008), however, there are no strong constraints on the time evolution of dark energy at present. Thus, evolving models of dark energy remain as alternative candidates for dark energy. Many non-cosmological constant models have been suggested for dark energy, including scalar field quintessence models, modifications of the Einstein framework of gravity, *etc.* (see reviews Sahni & Starobinsky 2000; Carroll 2001; Peebles & Ratra 2003; Copeland *et al.* 2006; Nojiri & Odinstov 2007; Sahni & Starobinsky 2006; Frieman *et al.* 2008, and references therein), but as of now there is no clear consensus on the nature on dark energy. An interesting class of models which have been suggested in the literature are early dark energy (EDE) models, in which the early universe contained a substantial amount of dark energy. Geometric probes of dark energy put strong constraints on the present-day nature of dark energy, and these constraints are expected to improve with future surveys. However, very little is known as to the nature of dark energy at early times due to paucity of data beyond redshifts of few. It has thus been hypothesized that even

if dark energy at present behaves like the cosmological constant, in the past it could have had completely different behavior, leading to the idea of the EDE models. Different facets of these models have been studied in recent works (Dodelson *et al.* 2000; Skordis & Albrecht 2002; Doran & Robbers 2006) and references therein, and have been analyzed with respect to observations extensively in recent times in (Linder & Robbers 2008; Francis *et al.* 2008; Grossi & Springel 2009; Fedeli *et al.* 2009; Xia & Viel 2009; Jennings *et al.* 2010; Alam 2010; de Putter *et al.* 2010). Current data places some constraints on these models, but does not rule them out. In this work we use a parameterization of the equation of state of dark energy to study the possibility of constraining EDE models using future large scale structure surveys.

Ground and space-based telescopes targeting clusters in microwave [Atacama Cosmology Telescope (ACT) (Hincks *et al.* 2009), the South Pole Telescope (SPT) (Staniszewski *et al.* 2009) and Planck <sup>1</sup>] have begun operation, or will return data shortly. Also current (Ebeling *et al.* 2010) and future missions have been planned for detecting clusters in X-ray waveband (Predehl *et al.* 2007). It has been recognized for some time now, that galaxy cluster surveys in X-ray or microwave via Sunyaev-Zel'dovich (SZ) effect could be precision probes of cosmological parameters, in particular the dark energy density and its equation of state parameter (Haiman *et al.* 2001). This is because redshift distribution of massive clusters is exponentially sensitive to the growth of structure history of the universe, which in turn, bears the signature of dark energy. The presence of early dark

Electronic address: ujjaini@lanl.gov  
Electronic address: zarija@lanl.gov  
Electronic address: sumanb@lanl.gov

<sup>1</sup> <http://www.rssd.esa.int/index.php?project=Planck>

energy reduce structure formation, consequently the cluster abundances reduce. Thus cluster counts can provide a smoking gun probe for detecting early dark energy. For example, (Mantz *et al.* 2010) have used a flux limited X-ray cluster data to constrain early dark energy component assuming the redshift of transition between 0 to 1. The current generation of SZ surveys will also measure the power spectrum of the cosmic microwave background with an unprecedented accuracy down to scales of 1 arc-min. The SZ surveys have started measuring the SZ power spectrum which is the dominant signal at scales of few *arc-min* (1; Fowler *et al.* 2010). The amplitude of the SZ power spectrum is proportional to the total number of objects that have formed and hence is extremely sensitive to the amount of dark energy present at early epoch.

The paper is organized as follows. In Section 2 we explain the early dark energy formalism and model used for this analysis. Section 3 expounds the nature of X-ray and microwave observations and mass-observable scaling relations. In section 4 we show predictions from current and future observations, comparing our EDE models to a fiducial  $\Lambda$ CDM cosmology. Finally, section 5 is devoted to conclusions and discussion.

## 2. EARLY DARK ENERGY

Dark energy perturbations for dynamic dark energy models have been studied in a number of works, usually under the formalism of a minimally coupled scalar field (See Ma *et al.* 1999; Hwang & Noh 2001; Hu 2002; Malquarti & Liddle 2002; Weller & Lewis 2003; Bean & Dore 2004; Dutta & Maor 2007; Mota *et al.* 2007; Novosyadlyj & Sergijenko 2008; Jassal 2009, and references therein). In this work we follow the formalism of (Weller & Lewis 2003). First order perturbations in a homogeneous and isotropic large scale universe described by the Friedman-Lemaitre-Robertson-Walker (FLRW) metric take the form

$$ds^2 = a^2(\eta) \left[ (1 + 2\Psi(\mathbf{x}, \eta))d\eta^2 - (1 + 2\Phi(\mathbf{x}, \eta))\delta_{\alpha\beta}dx^\alpha dx^\beta \right], \quad (1)$$

where  $\eta$  is the conformal time,  $\mathbf{x}$  is the length element,  $a(\eta)$  is the scale factor, and  $\Phi, \Psi$  are the Bardeen potentials. If proper isotropy of the medium is zero, then  $\Phi = -\Psi$ .

Along with the matter and radiation components, we consider dark energy to be an additional fluid component, so that the dark energy perturbations are characterized by an equation of state and an adiabatic sound speed–

$$w_{DE} = \frac{P_{DE}}{\rho_{DE}} \quad (2)$$

$$c_{a,DE}^2 = \frac{\dot{P}_{DE}}{\dot{\rho}_{DE}}. \quad (3)$$

Defining the frame-invariant quantity  $c_{s,i}^2$  (the fluid sound speed in the frame comoving with the fluid), the evolution equations for a fluid with equation of state  $w_i = p_i/\rho_i$ , and adiabatic speed of sound  $c_{a,i}^2 = \dot{p}_i/\dot{\rho}_i$ , can be written as (prime denotes derivative with respect to  $\eta$ )

$$\delta'_i = -3\mathcal{H}(c_{s,i}^2 - w_i)\delta_i - 9\mathcal{H}^2(c_{s,i}^2 - c_{a,i}^2)(1 + w_i)\frac{v_i}{k} - (1 + w_i)kv_i - 3(1 + w_i)\Psi' \quad (4)$$

$$v'_i = -\mathcal{H}(1 - 3c_{s,i}^2)v_i + \frac{kc_{s,i}^2\delta_i}{(1 + w_i)} - kA, \quad (5)$$

where  $\mathcal{H} = a'/a$  is the conformal Hubble parameter and  $A$  is the acceleration ( $A = 0$  in the synchronous gauge,  $A = -\Psi$  in

the Newtonian gauge). Adiabatic initial conditions are considered. For the matter component,  $w_m = c_a^2 = c_s^2 = 0$ . For the dark energy component, a fluid with varying  $w_{DE} \geq -1$  has  $c_{a,DE}^2 = w_{DE} - [dw_{DE}/d(\ln a)]/3(1 + w_{DE})$ . For scalar field like dark energy models,  $c_{s,DE}^2 = 1$ . For a more general class of models, such as k-essence,  $c_{s,DE}^2$  could be variable as well.

If we consider dark energy without perturbations, the quantities  $\delta_{DE}, \delta'_{DE} = 0$ , and the matter density contrast is given by

$$\delta_m'' - \mathcal{H}\delta_m' - 4\pi G\rho_m\delta_m = 0, \quad (6)$$

thus the dark energy component appears only in the damping term, so that a non-negligible amount of dark energy would lead simply to a suppression of clustering of matter at large scales. Not taking into account the dark energy perturbations can lead to gauge dependent results, as shown in (Park *et al.* 2009), in this paper we have used the commonly used comoving gauge. If dark energy perturbations are included self-consistently, the results are gauge-independent.

To study EDE models under this formulation, we consider a  $w$ -parameterization which may represent a large class of varying dark energy models (Corasaniti *et al.* 2003)

$$w(a) = w_0 + (w_m - w_0) \frac{1 + e^{a_t/\Delta_t}}{1 + e^{-(a-a_t)/\Delta_t}} \frac{1 - e^{-(a-1)/\Delta_t}}{1 - e^{1/\Delta_t}}, \quad (7)$$

where  $w_0$  is the equation of state of dark energy today,  $w_m$  is the equation of state in the matter dominated era,  $a_t$  is the scale factor at which the transition between  $w_0$  and  $w_m$  takes place, and  $\Delta_t$  is the width of the transition. For studying EDE models with this parameterization, we choose  $w_m > -0.1$ , to ensure the presence of adequate amount of dark energy at early times.

Current data puts impressive constraints on the values of these parameters (see Alam 2010), however, many interesting EDE models still fall in the acceptable range. We choose two such EDE models in order to study the possibility of constraining these models further using future observations. The models chosen are

- Model 1 :  $w_0 = -1.0, w_m = -0.05, a_t = 0.17, \Delta_t = 0.17$ ;
- Model 2 :  $w_0 = -0.9, w_m = -0.05, a_t = 0.1, \Delta_t = 0.1$ .

Model 1 behaves like  $\Lambda$ CDM at present, while Model 2 has a higher value of the equation of state at present. We compare the results for these models with those for a  $\Lambda$ CDM model with identical values for the non-dark energy parameters. The non-dark energy parameters are chosen from the WMAP7 CMB+BAO+HST best-fit, e.g.,  $\Omega_b h^2 = 0.0226, \Omega_c h^2 = 0.1123, h = 0.704, n_s = 0.963$ , as well as other parameters such as the scalar amplitude  $A_s$  and the reionization optical depth  $\tau$  (Komatsu *et al.* 2009). We modified the publicly available COSMOMC code (Lewis & Bridle 2002) for generating the transfer functions, and therefore the power spectrum at different redshifts for these models.

Figure 1 shows the behavior of the equation of state of dark energy, and the matter power spectrum at redshift  $z = 0$  for these two models. For comparison we also plot the results for the matter power spectrum when dark energy perturbations are not considered. We see that when the perturbations are not considered, the EDE matter power spectrum, although there is a suppression the matter power spectrum, this effect is negligible, and for both models the matter power spectrum is very close to that for  $\Lambda$ CDM. However, when the perturbations are considered, the matter power spectrum is significantly different from  $\Lambda$ CDM, resulting in a  $\sigma_8 = 0.74$  for EDE1, and a

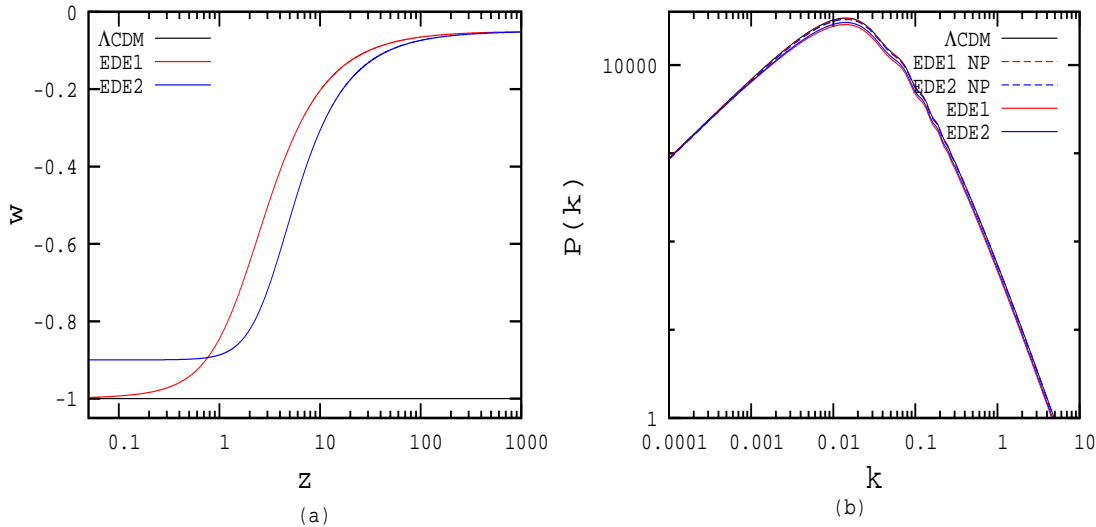


FIG. 1.— Equation of state (panel (a)) and matter power spectrum at  $z=0$  (panel (b)) for EDE models with  $w_0 = -1.0, w_m = -0.05, a_t = 0.17, \Delta_t = 0.17$  (EDE1, red lines), and with  $w_0 = -0.9, w_m = -0.05, a_t = 0.1, \Delta_t = 0.1$  (EDE2, blue lines). The black line in each panel represents the corresponding  $\Lambda$ CDM model, in panel (b), the dashed lines represent EDE without DE perturbations, while the solid lines represent EDE with perturbations.

$\sigma_8 = 0.76$  for EDE2, whereas the  $\Lambda$ CDM has a  $\sigma_8 = 0.81$ . This behavior is typical of EDE models with rapid and large transition of the equation of state. This translates to a rapid change in the dark energy perturbations at high scales (low  $k$ ), thus to an enhancement in the transfer function at low  $k$ . When normalized to the CMB scale, this effect shows up as an apparent suppression of power at high  $k$ , and therefore a low  $\sigma_8$ . The effect is stronger in EDE1 (i.e. lower  $\sigma_8$ ) because the difference between the equation of state at present and in the matter dominated era in this case is larger. Further details on how the change in equation of state affects the dark energy perturbations can be found in paper I (Alam 2010).

### 3. OBSERVATIONS

Paper I (Alam 2010) explores effects of early dark energy on CMB power spectrum and other current observations; here we focus on forthcoming large-scale structure probes. We consider the influence of EDE on cluster counts and SZ power spectrum.

#### 3.1. Cluster Counts

Redshift evolution of cluster abundance provides a valuable insight into global dynamics of the universe. This abundance is sensitive to both expansion and growth history of the universe, and as such can be used to constrain standard cosmological parameters like  $\sigma_8$  or  $\Omega_{0m}$  (see, e.g. Haiman et al. 2001), but also to explore possible mechanisms for observed acceleration, like modifying the law of gravity.

For a spatially flat cosmologies considered here ( $\Omega_{\kappa} \equiv 0$ ), all-sky number of objects more massive than  $M_{min}$  in a redshift bin is:

$$N(z) = \int_{M_{min}}^{\infty} \int_{z_1}^{z_2} \frac{4\pi r^2(z) dr(z)}{dz} \frac{dn(M, z)}{dM} dz dM, \quad (8)$$

where the first term is the comoving volume, and the second is the differential mass function.

From numerical simulations, we have a good quantification of the halo mass function. Although its precision is still not

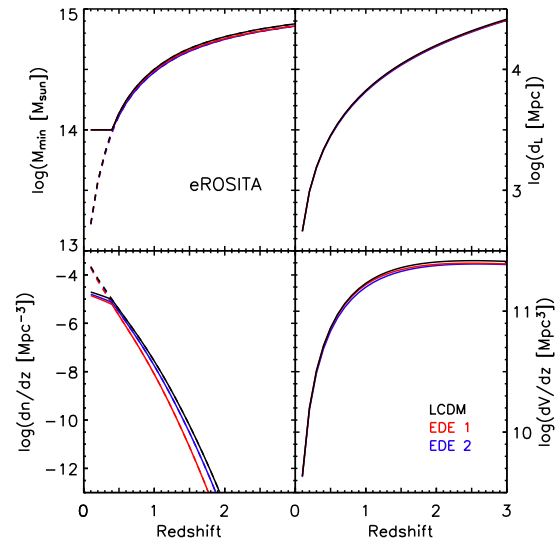


FIG. 2.— eROSITA survey, from upper left panel in clockwise direction: minimal detectable mass (dashed line shows instrument capability, solid line shows minimal mass for galaxy clusters only with mass threshold of  $10^{14} M_{\odot}$ ), luminosity distance, comoving volume element covered by the survey, and comoving cluster abundance as a function of redshift.

at the level needed to make it insignificant for future cosmological parameter studies (Cunha & Evrard 2009; Wu et al. 2009), that will not be relevant here as we want to explore the relative difference between our EDE models and the fiducial  $\Lambda$ CDM cosmology. The important point, on which we rely here, is that the mass function can be presented in a *universal* form, where the cosmology dependence comes from the linear power spectrum, and the linear growth factor. At a 20% level (often better than that), it is indeed proven to be the case, for many different cosmological models (Jenkins et al. 2001; Linder & Jenkins 2003; Jennings et al. 2010; Bhattacharya et al. 2010) and for a wide range of redshifts (Heit-

mann et al. 2006; Lukić et al. 2007; Reed et al. 2007). Since we are interested in modeling X-ray and SZ observations, we will use mass function of halos defined as spheres enclosing a given overdensity, defined with respect to the critical density for the closure,  $\rho_c$  (for analysis of different halo definitions see, e.g. White 2002; Lukić et al. 2009).

One way of detecting groups and clusters of galaxies is via weak lensing maps (Marian & Bernstein 2006); this approach is appealing as masses are probed directly there, but on a downside the method can probe only the most massive systems, and only within limited redshifts (as galaxy shapes are very hard to measure beyond  $z \sim 1$ ). Promising alternatives to the weak lensing are mass measures through Sunyaev-Zel'dovich effect (e.g. Carlstrom et al. 2002), X-ray emission (e.g. Kravtsov et al. 2006), and galaxy richness (High et al. 2010). For these, indirect mass measurements, one first has to connect cluster mass to a relevant observable for a given survey, like X-ray flux (Mantz et al. 2010) or integrated Compton  $y$ -parameter (Vanderlinde et al. 2010; Sehgal et al. 2010). In this paper we will focus on X-ray and SZ surveys, and in the following we explain scaling relations we use.

In the self-similar theory (Kaiser 1986, 1991), temperature of the intracluster medium scales with gravitational potential ( $T \propto M/R$ ), and enclosed mass is  $M \propto R^3$ . This self-similar scaling was confirmed in hydrodynamical simulations (Mathiesen & Evrard 2001; Borgani et al. 2004; Kravtsov et al. 2006), as well as in observations (Vikhlinin et al. 2009). In the following, we will use  $M-T$  relation from Mathiesen & Evrard (2001):

$$\frac{M_{200}}{M_\odot h^{-1}} = 10^{15} \left( \frac{kT}{4.88 \text{keV}} \right)^{3/2} E(z)^{-1}; \quad E(z) \equiv H(z)/H_0. \quad (9)$$

We use the above relation, as it relates  $M_{200}$  to the bolometric luminosity. While X-ray scaling relations are much tighter for  $M_{500}$  (Kravtsov et al. 2006), here we want to use the same mass for both X-ray and SZ estimates, and whether it is the best observational approach is not of concern here.

Self-similar theory fails to correctly predict  $T-L$  relation (Markevitch 1998; Allen & Fabian 1998), and thus mass-luminosity relation is inaccurate as well. The departure from self-similarity is due to excess entropy in cluster cores which prevents gas from being compressed to very high densities (Ponman et al. 1999, Finoguenov et al. 2002). Therefore, in the following we will use  $M-L$  relation from Bartelmann & White (2003):

$$L = 1.097 \times 10^{45} \left[ \frac{M_{200}}{10^{15} M_\odot h^{-1}} E(z) \right]^{1.554} \text{ erg/s} \quad (10)$$

X-ray observations are sensitive in a given energy band, whose flux is:

$$S_b = \frac{L_X f_b}{4\pi d_L(z)^2}, \quad (11)$$

where  $f_b$  is the band correction and  $d_L(z)$  is luminosity distance to a cluster:

$$d_L(z) = \frac{c(1+z)}{H_0} \int_0^z \frac{dz'}{E(z')}. \quad (12)$$

Emission from the intracluster medium is predominantly thermal bremsstrahlung, but for  $T < 2\text{keV}$  line emission from metals (clusters have metallicity  $\sim 0.3Z_\odot$ ) becomes non-negligible (Sarazin 1986). Thus, to calculate  $f_b$  we use

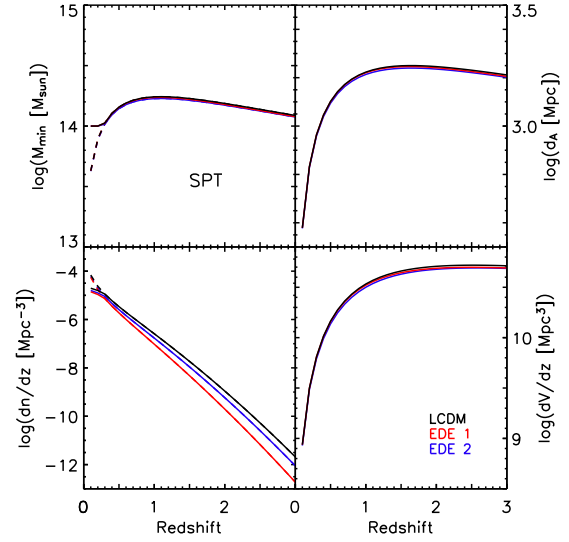


FIG. 3.— South Pole SZ survey, from upper left panel in clockwise direction: minimal detectable mass (dashed line shows instrument capability – same as in Figure 2), angular diameter distance, comoving volume element covered by the survey, and comoving cluster abundance as a function of redshift.

XSPEC package (Arnaud 1996) and we assume Raymond-Smith (1977) plasma model for cluster emission. As the band correction depends on the plasma temperature, we solve iteratively for minimum mass and corresponding temperature using XSPEC and equation 9. Galactic absorption is modeled with constant column density of  $n_H = 10^{21} \text{cm}^{-2}$ , roughly corresponding to Galactic mid-latitudes. In observational analysis one would use appropriate  $n_H$  for the line of sight to each cluster, and column density will generally be smaller than our number for high latitudes, and larger for low latitudes.

For the Sunyaev-Zel'dovich observations, one has to relate Compton  $y$  parameter (integrated over the solid angle) to the mass of an object. Furthermore, it is necessary to renormalize such relation to the directly observable SZ flux. In Fedeli et al. (2009), this was done using Sehgal et al. (2007)  $Y_{200}-M_{200}$  relation, and assumption that SZ signal outside cluster virial radius can safely be neglected, resulting in relation:

$$S_\nu = \frac{6.763 \times 10^7 \text{mJy}}{(d_A(z)/1 \text{Mpc})^2} \left( \frac{M_{200}}{10^{15} M_\odot} \right)^{1.876} |f(\nu)| E^{2/3}(z). \quad (13)$$

Here,  $d_A$  is angular diameter distance to the object, and  $f(\nu)$  is spectral signature of the thermal SZ effect:

$$f(\nu) = \frac{x^4 e^x}{(e^x - 1)^2} \left[ x \frac{e^x + 1}{e^x - 1} - 4 \right]; \quad x \equiv \frac{h\nu}{kT_\gamma}, \quad (14)$$

and  $T_\gamma$  is the CMB temperature.

### 3.2. Sunyaev-Zeldovich Power Spectrum

The current generation of CMB experiments will measure the power spectrum of the cosmic microwave background with an unprecedented accuracy down to scales of 1 arc-min. While the primary CMB fluctuations dominate the power spectrum at a degree scale, at scales of few arcminutes the secondary fluctuations arising from the SZ effect and lensing of the CMB becomes the dominant signal.

Predictions for the SZ power spectrum amplitude  $C_{l,SZ}$  (henceforth  $C_l$ ) can be made using the halo model and estimates of the radial pressure profile of intra-cluster gas.

Assuming that the cluster gas resides in hydrostatic equilibrium in the potential well of the host dark matter halo, (Komatsu & Seljak 2002) demonstrated that the ensemble averaged power spectrum amplitude  $C_l$  has an extremely sensitive dependence on  $\sigma_8$  where  $C_l \propto \sigma_8^7 (\Omega_b h^2)^2$ . The kinetic SZ power spectrum contribute roughly 10% to the total SZ angular power spectrum and hence we consider only the thermal component of the SZ power spectrum (tSZ hereafter) here. The cosmological information of the tSZ power spectrum comes from the total number of halos of mass  $M \geq 10^{13} M_\odot/h$  in the survey area. Thus the SZ power spectrum contains a significant contribution from low mass clusters and group-mass objects. Note that measurements of the mass function usually probe only massive halos ( $M \geq 10^{14} M_\odot$ ) and not group size halos.

The SZ power spectrum can be calculated by simply summing up the squared Fourier-space SZ profiles,  $\tilde{y}(M, z, \ell)$  of all clusters:

$$C_\ell = g_\nu^2 \int dz \frac{dV}{dz} \int d \ln M \frac{dn(M, z)}{d \ln M} \tilde{y}(M, z, \ell)^2 \quad (15)$$

where  $V(z)$  is the comoving volume per steradian and  $n(M, z)$  is the number density of objects of mass  $M$  at redshift  $z$ .  $g_\nu$  is the frequency factor of the SZ effect. In this study, we show the power spectrum at 150 GHz where  $g_\nu = -1$ . Note that whilst this calculation assumes that clusters are Poisson distributed, (Shaw et al. 2009) have shown that including halo clustering modifies the power spectrum (compared to the Poisson case) by less than 1%.

The number density of halos  $n(M, z)$  can be calculated for a  $\Lambda$ CDM cosmology using the fitting functions provided by (Jenkins et al. 2001) and more recently (Tinker et al. 2008). For the SZ profiles (also mass and redshift dependent), previous studies have frequently used either a simple  $\beta$ -model or the hydrostatic model of (Komatsu & Seljak 2002). Note that both models simply assume that the gas resides in hydrostatic equilibrium in the potential well of an NFW-like halo (and is isothermal in the case of the  $\beta$ -model). Neither model accounts for the fraction of hot gas that will have cooled and been converted into stars or any non-thermal energy input into the ICM. As shown in (White et al. 2002; Bhattacharya et al. 2008; Battaglia et al. 2010), these effects change the SZ power spectrum by 10-30%. One possible way to include the uncertainty in gas physics is the semi-analytic approach of modeling gas physics (Bode et al. 2007; Bode et al. 2009; Shaw et al. 2010) and calibration the parameters using X-ray observations of individual clusters. The other source of uncertainty is the non-gaussian nature of the SZ power spectrum (Shaw et al. 2009). All these effects needs to be accounted for precision modeling of the power spectrum. This will be essential to harness the full merit of the upcoming datasets. In the current study we choose to use the model by (Komatsu & Seljak 2002) to assess the impact of dark energy on the SZ power spectrum.

## 4. RESULTS

### 4.1. Cluster counts

We consider two observational campaigns: upcoming X-ray survey eROSITA, and ongoing South Pole SZ survey. The first one, due in 2012, will cover almost half a sky ( $f_{sky} \approx 0.49$ ), and have flux limit of  $F_{min} = 3.3 \times 10^{-14} \text{ergs}^{-1} \text{cm}^{-2}$  in energy band [0.5, 5.0] keV. South Pole Telescope will scan 4000 square degrees ( $f_{sky} \approx 0.1$ ) with limit of  $S_{min} \approx 5 \text{mJy}$  at

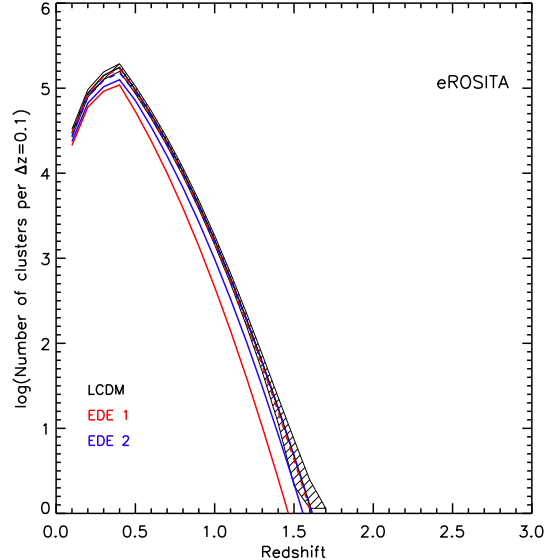


FIG. 4.— Expected redshift distribution of galaxy clusters for eROSITA Telescope. In black is our fiducial  $\Lambda$ CDM model, red and blue are EDE1, and EDE2, respectively, and in dashed lines we show results of EDE models when perturbations are neglected. Shaded regions are statistical Poisson errors plus 10% systematic error coming from non-universality of the mass function.

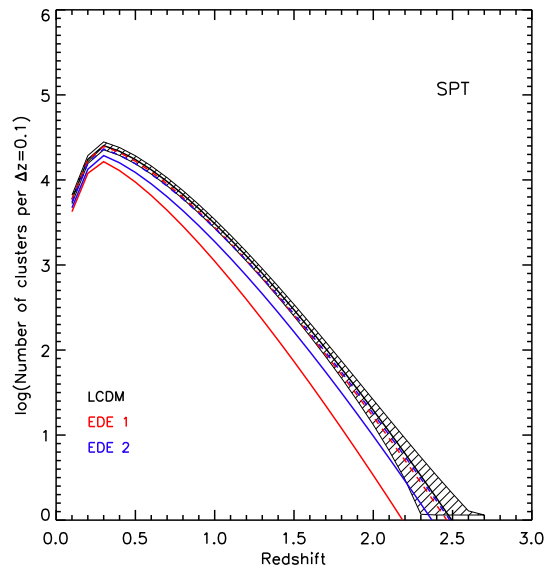


FIG. 5.— The same as Fig. 4, but for the South Pole Telescope.

frequency  $\nu_0 = 150 \text{Hz}$ . Using mass-observable scaling relations described in section 3.1 we can find minimum detectable mass for each survey, as well as redshift volume element being observed (Figs. 2 and 3). For the theoretical prediction of cluster abundance, we use Tinker et al. (2008) mass function for the overdensity of  $200\rho_c$  ( $\Delta \approx 778$  in their notation), and we use their fitting formulas for the parameters of  $f(\sigma)$  as the function of  $\log \Delta$ . Total number density of objects with masses above the given threshold as predicted by Tinker et al. (2008) is shown in lower left panels of Figures 2 and 3, for eROSITA and SPT survey, respectively.

Figures 4 and 5 show expected redshift distribution of galaxy clusters for the cosmologies considered here, where

we have taken redshift bins of  $\Delta z = 0.1$ . As expected, SZ survey can detect meaningful number of clusters up to higher redshift, but has fewer objects at lower redshifts, due to the smaller sky coverage. Shaded area shows Poisson errorbar plus a systematic 10% uncertainty which describes our confidence in universal formula of the mass function. Dashed lines show expectations for EDE models if perturbations would be neglected. We see that presence of perturbations significantly affect growth of structure in the Universe, effectively reducing  $\sigma_8$ . Since amount of this reduction is redshift dependent, it is not possible to mimic it with  $\Lambda$ CDM cosmology with different  $\sigma_8$  (i.e. it is possible to mimic it at a particular redshift, but not at a redshift range). Most importantly, we see that perturbations cannot be neglected when considering predictions from dynamical EDE models.

Finally, Figures 4 and 5 showcase that future large-scale structure results will be able to constrain EDE models significantly better than is currently the case. Both EDE1 and EDE2 models, which represent models which are (a) indistinguishable from  $\Lambda$ CDM at present (EDE1), or (b) at the upper limit of  $w_0$  (EDE2), are distinguishable from  $\Lambda$ CDM cosmology with high significance ( $2\sigma$  or more). Constraining power is larger on the EDE1 model which behaves the same as  $\Lambda$ CDM today but has a later transition from EDE like behavior (at redshift  $z \simeq 5$ ), as compared to the EDE2 model which is different from  $\Lambda$ CDM today but has a much earlier transition from EDE like behavior (at redshift  $z = 9$ ). Thus the cluster counts may constrain not only the current equation of state of dark energy, but also the redshift at which transition from EDE behavior occurs.

#### 4.2. SZ power spectrum

In this section, we show the impact of the dark energy perturbation on the SZ power spectrum. The presence of perturbations in the dark energy changes the transfer function, volume factor and the growth function of the universe, consequently the abundance of the halos changes. Since SZ power spectrum is proportional to the total abundance of the halos that have formed in the universe and volume of the universe, it depends strongly on the perturbations of dark energy. The impact of different early dark energy models on the SZ power spectrum is shown in figure 6. To assess the merit of the upcoming datasets to constrain early dark energy we assume two fiducial surveys:

- 1) Planck like full sky survey: We assume 75% of the full sky coverage to exclude contaminations due to galactic foregrounds,  $7'$  resolution and  $7 \mu K$  per pixel as the sensitivity.
- 2) ACT/SPT like higher resolution surveys: We assume a coverage of  $4000 \text{ deg}^2$ ,  $1.2'$  angular resolution and a sensitivity of  $20 \mu K$  per pixel.

The error on the SZ power spectrum for closely separated bins of size  $\Delta l$  in  $l$  space can be written as

$$\sigma^2(C_l) = f_{sky}^{-1} \left[ \frac{2C_l^2}{(2l+1)\Delta l} + \frac{2}{(2l+1)\Delta l} \left( f_{sky} w^{-1} \exp \left[ \frac{l^2 \theta_{fwhm}^2}{8 \ln 2} \right] \right)^2 + \frac{T_{ll}}{4\pi} \right] \quad (16)$$

where  $f_{sky}$  is the fraction of the sky covered by the assumed surveys,  $w^{-1} = [\sigma_{pix} \theta_{fwhm} / T_{CMB}]^2$ ,  $\sigma_{pix}$  is the noise per pixel,  $\theta_{fwhm}$  is the resolution at full width at half maximum

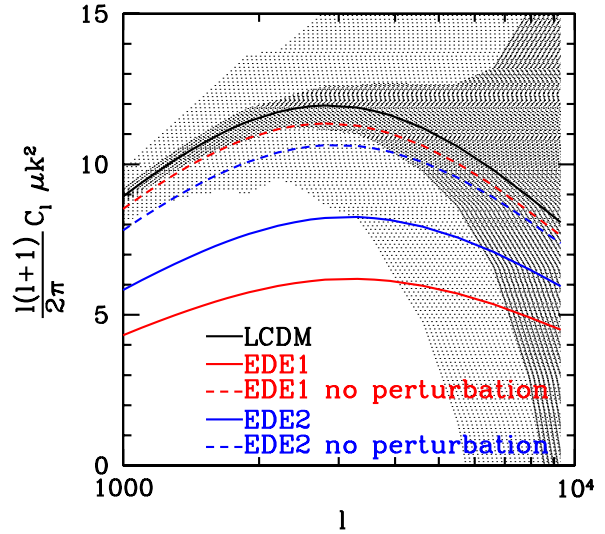


FIG. 6.— The impact of dark energy perturbations on the SZ power spectrum. Different early dark energy models are explained in section 2. The error bars represent a Planck like full sky survey and ACT/SPT like higher resolution survey. The error bars include cosmic variance including the non-gaussian contribution from the SZ trispectrum and the resolution of the surveys. We assume perfect removal of astrophysical contaminations from infrared and radio galaxies and primary CMB, assuming a gaussian beam,  $T_{CMB}$  is the CMB temperature (Jungman et al. 1996).

The trispectrum  $T_{ll}$  (Poisson term) is given by

$$C_\ell = g_\nu^4 \int dz \frac{dV}{dz} \int d \ln M \frac{dn(M, z)}{d \ln M} \bar{y}(M, z, \ell)^4 \quad (17)$$

As shown in fig. 6, the upcoming measurements of SZ power spectrum will be able to distinguish between  $\Lambda$ CDM and different early dark energy models (that are not ruled out by current observations) with high significance. As in the case of the galaxy cluster counts, the SZ power spectrum is also sensitive to the redshift of transition from EDE-like to present day  $\Lambda$ CDM-like behavior. Current constraints on the redshift and width of transition are  $z_t \gtrsim 4$ ,  $\Delta_t \lesssim 0.2$  (Alam 2010), while future observations of SZ power spectrum may even rule out EDE models with  $z_t \gtrsim 9$ ,  $\Delta_t \lesssim 0.1$  (EDE2). These results are of course for a fixed value of other non-dark energy parameters, and we expect degeneracies with these in a full analysis. In the next section we attempt to constrain the EDE parameters using future simulated SZ power spectrum measurements and cluster counts.

#### 4.3. Likelihood analysis

In this section we study the effect of the degeneracies between the different cosmological parameters for EDE models. We simulate the data according to WMAP7+BAO+ $H_0$   $\Lambda$ CDM model (Komatsu et al. 2009). We generate the primary CMB TT power spectrum simulated to match the Planck survey resolution and sky coverage. We also simulate the SZ power spectrum data as obtainable from ACT/SPT surveys with the survey parameters discussed in detail in section 4.2. For studying the cluster data, we simulate SPT survey, assuming Tinker et al. (2008) number density of clusters; the details are given in section 4.1. The results for eRosita are expected to be similar.

Typically, the cluster data alone is not enough to break the degeneracies between different parameters and we need

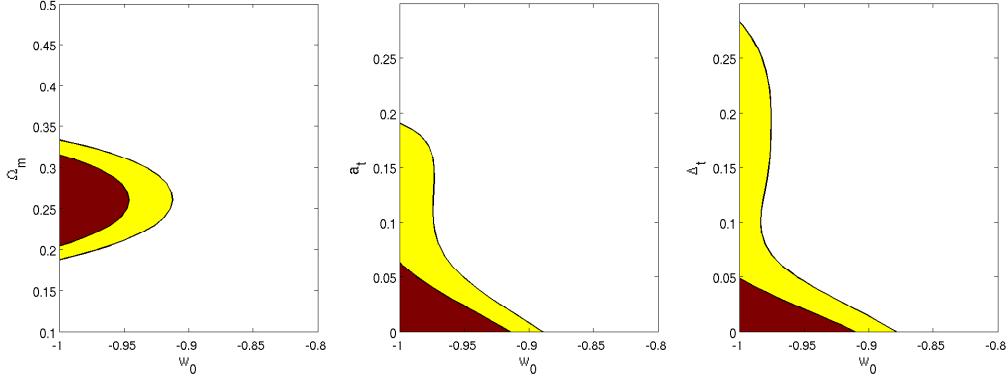


FIG. 7.— Confidence levels for a combination of primary CMB power spectrum from Planck survey + cluster counts obtainable from ACT/SPT survey.

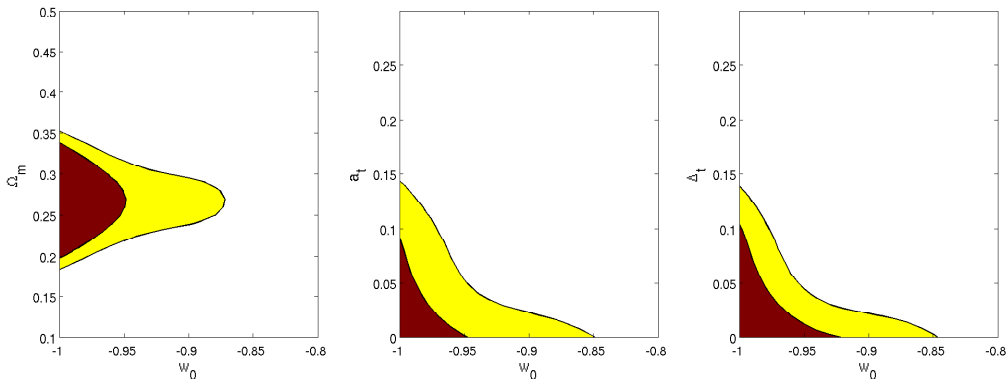


FIG. 8.— Confidence levels for a combination of primary CMB power spectrum from Planck survey + SZ power spectrum obtainable from ACT/SPT survey.

the constraints from the primary CMB power spectrum. We add CMB data in the form of scalar Cl's simulated as per Planck specifications. We also apply a Gaussian prior on  $H_0$  as  $H_0 = 70.4 \pm 3.6$  km/s/Mpc, where the error is consistent with the recent results of the Hubble constant from the SHOES (Supernovae and  $H_0$  for the Equation of State) program (Riess *et al.* 2009). We do not add any other possible future datasets such as the supernovae or Baryon Acoustic Oscillations.

In analyzing the data, we keep  $w_m \geq -0.1$  since we are interested in constraining models which have sufficient amount of dark energy at early times. The true  $\Lambda$ CDM model cannot be exactly reproduced by the EDE class of models since  $w_m \neq -1$ , but in the limit  $w_0 = -1, a_t \rightarrow 0$  ( $z_t \rightarrow \infty$ ),  $\Delta_t \rightarrow 0$  these models replicate  $\Lambda$ CDM-like behavior.

As shown in figure 7, CMB + cluster count analysis can constrain the EDE parameters to  $w_0 \lesssim -0.9, a_t \lesssim 0.2$  ( $z_t \gtrsim 4$ ),  $\Delta_t \lesssim 0.3$ , which implies that cluster counts + CMB can constrain any deviation from  $\Lambda$ CDM behavior upto at least  $z=4$ . For the SZ power spectrum data, we find that the EDE parameters are constrained to  $w_0 \lesssim -0.85, a_t \lesssim 0.15$  ( $z_t \gtrsim 5.5$ ),  $\Delta_t \lesssim 0.15$  (see figure 8). SZ power spectrum provide complementary information about dark energy parameters compared to cluster counts. For example, SZ power spectrum put tighter constraints on the dark energy transition parameters compared to cluster counts. The matter density is reasonably reconstructed for both the cluster counts and SZ power spectrum.

## 5. CONCLUSIONS

In this work, we have studied early dark energy models in light of future galaxy cluster data. We study two EDE models, both of which are allowed within the current observational constraints. The first model (EDE1) transits from EDE behavior at redshift  $z \gtrsim 5$  to  $\Lambda$ CDM-like behavior at present, while the second model (EDE2) transits at a higher redshift ( $z \simeq 9$ ) to an equation of state  $w_0 = -0.9$ , which is close to but not identical to  $\Lambda$ CDM. For both the models, as well as for the fiducial  $\Lambda$ CDM cosmology, we show the predictions for cluster abundance and SZ power spectrum. For that purpose, we consider two instruments – eROSITA for X-ray surveys, and ACT/SPT for SZ effect. We also do a likelihood analysis of data simulated replicating the SPT and eRosita survey specifications, along with the simulated Planck CMB data, to obtain the constraints on the EDE parameters from future surveys, and find that future galaxy cluster counts and SZ power spectrum can put competitive constraints on these parameters.

It is worth noting some apparent differences between our work here, and some other recent works on EDE signatures. For example, Fedeli *et al.* (2009) also considered several EDE models, but their cluster counts are higher than for the fiducial  $\Lambda$ CDM model, although  $\sigma_8$  for EDE models are commonly lower in their work (as it is the case here as well). That is because for their choice of EDE models Hubble parameters,  $E(z)$  differs significantly from the corresponding  $\Lambda$ CDM model. This affects minimum observable mass as a function of redshift; their EDE models have much lower mass threshold than  $\Lambda$ CDM, thus resulting in higher observable cluster counts. In contrast, we have chosen models which have  $E(z)$  similar to that of the corresponding  $\Lambda$ CDM model, to high-

light the difference coming from the perturbations rather than the background expansion. Similar difference from this work, due to the radical departure of  $E(z)$  from  $\Lambda$ CDM, can be seen in Waizmann & Bartelmann (2009), for the effects of EDE on SZ power spectrum. In some other cases differences can arise depending whether one uses low- $k$ , CMB normalization of the power spectrum as done here, or  $\sigma_8$  normalization as in Sadeh et al. (2007), although it is clear that a successful model has to fulfill both constraints.

We show that the inclusion of dark energy perturbations has a major effect on the matter power spectrum, therefore increasing the possibility of discriminating EDE models from  $\Lambda$ CDM using large scale structure probes. Neglecting the dark energy perturbations leads to severe underestimation of the imprint which the sharp transition in dark energy equation of state leaves on the dark energy perturbations and therefore on the matter power spectrum. We show that the models considered here which are allowed by the current observations can be ruled out using the future galaxy cluster probes. It is also interesting that both the cluster counts and the SZ power spectrum are sensitive to the redshift at which the transition between early and present day dark energy occurs. We expect

to put strong constraints on the equation of state of dark energy at present using low redshift geometric observables (such as the luminosity distance of type Ia SNe and Baryon Acoustic Oscillations peaks). These probes of geometry of the Universe, however, are insensitive to the high redshift behavior of dark energy. The galaxy cluster observables such as their redshift abundance and the SZ power spectrum, although at low redshift, are sensitive to the perturbations in the early dark energy models, and hence would be able to put constraints on the redshift of transition from EDE behavior to present-day,  $\Lambda$ CDM-like behavior. With the ongoing and future cluster surveys in microwave, optical and X-ray waveband, galaxy clusters will be able to provide strong constraints on the dynamical dark energy sector.

## 6. ACKNOWLEDGEMENTS

We thank Konstantin Borozdin, Salman Habib and Katrin Heitmann for useful discussions. We also thank the referee for his useful suggestions. The authors acknowledge support from Los Alamos National Laboratory and the Department of Energy via the LDRD program at LANL.

## REFERENCES

- Alam, U. 2010, *ApJ* 714, 1460  
 Allen, S. W. & Fabian, A. C. 1998, *Mon. Not. Roy. Ast. Soc.* 297, L57  
 Arnaud, K. A. 1996, *ASPC* 101, 17  
 Bartelmann, M. & White, S. D. M. 2003, *A&A* 407, 845  
 Battaglia, N., Bond, J. R., Pfrommer, C., Sievers, J. L., & Sijacki, D. 2010, *arXiv:1003.4256*  
 Bean, R., & Dore, O. 2004, *Phys. Rev. D* 69, 083503  
 Bhattacharya, S., Di Matteo, T., & Kosowsky, A. 2008, *Mon. Not. Roy. Ast. Soc.* 389, 34  
 Bhattacharya, S., Heitmann, K., White, M., Lukić, Z., Wagner, C., & Habib, S. 2010, *arXiv:1005.2239*  
 Bode, P., Ostriker, J. P., Weller, J., & Shaw, L. 2007, *ApJ* 663, 139  
 Bode, P., Ostriker, J. P., & Vikhlinin, A. 2009, *ApJ* 700, 989  
 Borgani, S. et al. 2004, *Mon. Not. Roy. Ast. Soc.* 348, 1078  
 Carlstrom, J. E., Holder, G. P., Reese, E. D. 2002, *ARA&A* 40, 643  
 Carroll, S. M. 2001, *Living Rev. Rel.* 4, 1  
 Copeland, E. J., Sami, M. & Tsujikawa, S. 2006, *Int. J. Mod. Phys. D* 15, 1753  
 Corasaniti, P. S., & Copeland, E. J. 2003, *Phys. Rev. D* 67, 063521  
 Cunha, C. E. & Evrard, A. E. 2009, *arXiv:0908.0526*  
 de Putter, R., Huterer, D., & Linder, E. V. 2010, *arXiv:1002.1311*  
 Dodelson, S., Kaplinghat, M., Stewart, E. 2000, *Phys. Rev. Lett.* 85, 5276  
 Doran, M., & Robbers, G. 2006, *J. Cosmol. Astropart. Phys.* 0606, 026  
 Dutta, S., & Maor, I. 2007, *Phys. Rev. D* 75, 063507  
 Ebeling, H., Edge, A. C., Mantz, A., Barrett, E., Henry, J. P., Ma, C. J., van Speybroeck, L. 2010, *Mon. Not. Roy. Ast. Soc.* 407, 83  
 Fedeli, C., Moscardini, L., & Bartelmann, M. 2009, *Astron. Astrophys.* 500, 667  
 Fowler, J. W. et al. 2010, *arXiv:1001.2934*  
 Francis, M. J., Lewis, G. F. & Linder, E. V. 2008, *Mon. Not. Roy. Ast. Soc.* 393, L31  
 Frieman, J., Turner, M., & Huterer, D. 2008, *Ann. Rev. Astron. Astrophys.* 46, 385  
 Grossi, M., & Springel, V. 2009 *Mon. Not. Roy. Ast. Soc.* 394, 1559  
 Haiman, Z., Mohr, J. J., & Holder, G. P. 2001, *ApJ*, 553, 545  
 Heitmann, K., Lukić, Z., Habib, S. & Ricker, P. M. 2006, *ApJ* 642, L, 85  
 High, F. W. et al. 2010, *arXiv:1003.0005*  
 Hincks, A. D., et al. 2009, *arXiv:0907.0461*  
 Hu, W. 2002, *Phys. Rev. D* 65, 023003  
 Hwang, J., & and H. Noh, H. 2001, *Phys. Rev. D* 64, 103509  
 Jassal, H. K. 2009 *Phys. Rev. D* 79, 127301  
 Jenkins, A. et al. 2001, *Mon. Not. Roy. Ast. Soc.* 321, 372  
 Jennings, E., Baugh, C. M., Angulo, R. E., & Pascoli, S. 2009, *Mon. Not. Roy. Ast. Soc.* 401, 2181  
 Jungman, G., Kamionkowski, M., Kosowsky, A., & Spergel, D. N. 1996, *Phys. Rev. D*, 54, 1332  
 Kaiser, N. 1986, *Mon. Not. Roy. Ast. Soc.* 222, 323  
 Kaiser, N. 1991, *ApJ* 383, 104  
 Komatsu, E. et al., 2010, *arXiv:1001.4538*  
 Komatsu, E., & Seljak, U. 2002, *Mon. Not. Roy. Ast. Soc.* 336, 1256  
 Kowalski, M. et al., 2008 *ApJ* 686, 749  
 Kravtsov, A. V., Vikhlinin, A. & Nagai, D. 2006, *ApJ* 650, 128  
 Lewis, A. & Bridle, S., 2002 *Phys. Rev. D* 66, 103511. Available at <http://cosmologist.info/cosmomc>  
 Linder, E. V., & Jenkins, A. 2003, *Mon. Not. Roy. Ast. Soc.* 346, 573  
 Linder, E. V., & Robbers, G. 2008 *J. Cosmol. Astropart. Phys.* 0806, 004  
 Lueker, M., et al. 2009, *arXiv:0912.4317*  
 Lukić, Z., Heitmann, K., Habib, S., Bashinsky, S. & Ricker, P. M. 2007, *ApJ* 671, 1160  
 Lukić, Z., Reed, D., Habib, S. & Heitmann, K. 2009, *ApJ* 692, 217  
 Ma, C-P, Caldwell, R. R., Bode, P., & Wang, L-M. 1999, *ApJ* 521, L-1  
 Malquarti, M., & Liddle, A. R. 2002, *Phys. Rev. D* 66, 123506  
 Mantz, A., Allen, S. W., Ebeling, H., Rapetti, D., & Drlica-Wagner, A. 2010, *MNRAS*, 406, 1773  
 Mantz, A., Allen, S. W., Rapetti, D., & Ebeling, H. 2010, *MNRAS*, 406, 1759  
 Marian, L. & Bernstein, G. M. 2006, *Phys. Rev. D* 73, 123525  
 Markevitch, M. 1998, *ApJ* 504, 27  
 Mathiesen, B. F. & Evrard, A. E. 2001, *ApJ* 546, 100  
 Mota, D. F., Kristiansen, J. R., Koivisto, T., & Groeneboom, N. E. 2007, *Mon. Not. Roy. Ast. Soc.* 382, 793  
 Nojiri, S., & Odintsov, S. D. 2007, *Int. J. Geom. Meth. Mod. Phys.* 4, 115  
 Novosyadlyj, B., & Sergijenko, O. 2008, *arXiv:0808.2098*  
 Park, C-G, Hwang, J-C, Lee, J-H, & Noh, H. 2009, *Phys. Rev. Lett.* 103, 151303  
 Peebles, P. J. E., & Ratra, B. 2003, *Rev. Mod. Phys.* 75, 559  
 Predehl, P., et al. 2007, *SPIE* 6686, 668617  
 Raymond, J. C. & Smith, B. W. 1977, *ApJ Suppl* 35, 419  
 Reed, D., Bower, R., Frenk, C. S., Jenkins, A. & Theuns, T. 2007, *Mon. Not. Roy. Ast. Soc.* 374, 2  
 Reiss, A. G., et al., 2009 *ApJ* 699, 539  
 Sadeh, S., Rephaeli, Y., Silk, J. 2007, *Mon. Not. Roy. Ast. Soc.*, 380, 637  
 Sahni, V., & Starobinsky, A. A. 2000, *Int. J. Mod. Phys. D* 9, 373  
 Sahni, V., & Starobinsky, A. A. 2006, *Int. J. Mod. Phys. D* 15, 2105  
 Sarazin, C. L. 1986, *RvMP* 58, 1  
 Sehgal, N., Trac, H., Huffenberger, K. & Bode, P. 2007, *ApJ* 664, 149  
 Sehgal, N., et al. 2010, *arXiv:1010.1025*  
 Shaw, L. D., Zahn, O., Holder, G. P., & Doré, O. 2009, *ApJ* 702, 368  
 Shaw, L. D., Nagai, D., Bhattacharya, S., & Lau, E. T. 2010, *arXiv:1006.1945*  
 Skordis, C., & Albrecht, A. 2002, *Phys. Rev. D* 66, 043523  
 Staniszewski, Z., et al. 2009, *ApJ* 701, 32  
 Tinker, J. et al. 2008, *ApJ* 688, 709  
 Vanderlinde, K., et al. 2010, *ApJ*, 722, 1180  
 Vikhlinin, A. et al. 2009, *ApJ* 692, 1060  
 Waizmann, J.-C. & Bartelmann, M. 2009, *A&A*, 493, 859  
 Weller, J., & Lewis, A. M. 2003, *Mon. Not. Roy. Ast. Soc.* 346, 987  
 White, M. 2002, *ApJ Suppl*, 143, 241  
 White, M., Hernquist, L., & Springel, V. 2002, *ApJ* 579, 16  
 Xia, J-Q., & Viel, M. 2009 *J. Cosmol. Astropart. Phys.* 0904, 002



Wu, H-Y., Zentner, A. R., Wechsler, R. H. 2009, [arXiv:0910.3668](https://arxiv.org/abs/0910.3668)